Submitted to Physical Review B

LBL-2210
Preprint

c. 1

COHERENT ENERGY MIGRATION IN SOLIDS II. SPIN RESONANCE ABSORPTION IN COHERENT WAVE PACKET STATES AND THE EFFECTS OF PHONON-EXCITON SCATTERING

C.B. Harris and M.D. Fayer

August 1973

Prepared for the U.S. Atomic Energy Commission
under Contract W-7405-ENG-48

For Reference

Not to be taken from this room

LAWRENCE BERKELEY LABORATORY
UNIVERSITY OF CALIFORNIA
BERKELEY

LBL-2210

DISCLAIMER

This document was prepared as an account of work sponsored by the United States Government. While this document is believed to contain correct information, neither the United States Government nor any agency thereof, nor the Regents of the University of California, nor any of their employees, makes any warranty, express or implied, or assumes any legal responsibility for the accuracy, completeness, or usefulness of any information, apparatus, product, or process disclosed, or represents that its use would not infringe privately owned rights. Reference herein to any specific commercial product, process, or service by its trade name, trademark, manufacturer, or otherwise, does not necessarily constitute or imply its endorsement, recommendation, or favoring by the United States Government or any agency thereof, or the Regents of the University of California. The views and opinions of authors expressed herein do not necessarily state or reflect those of the United States Government or any agency thereof or the Regents of the University of California.

COHERENT ENERGY MIGRATION IN SOLIDS

II. SPIN RESONANCE ABSORPTION IN COHERENT WAVE PACKET STATES AND THE EFFECTS OF PHONON-EXCITON SCATTERING

C. B. Harris* and M. D. Fayer

Inorganic Materials Research Division, Lawrence Berkeley Laboratory
and Department of Chemistry; University of California
Berkeley, California 94720

*Alfred P. Sloan Fellow

Abstract

A model is presented which describes the effects of phonon-exciton scattering on the coherent migration of Frenkel excitons. The development is such that it provides for experimental verification through the use of electron spin resonance techniques. Both qualitative and quantitative information on the mode of exciton migration, the rate of phonon-exciton scattering, and the temperature dependence of phonon-exciton scattering at low temperatures are obtainable from the model. One-dimensional triplet excitons are considered specifically although the treatment is applicable to other phenomena such as impuriton migration. Three cases are treated. In the first, the exciton dispersion is taken to be much smaller than the acoustic phonon dispersion. In the second, the exciton and phonon dispersions are taken to be approximately equal, and in the third case, the exciton dispersion is taken to be much larger than the acoustic phonon dispersion. In each case, the possibility of long range energy migration is considered and is related to experimental observables. In addition, the effects of selective spin-orbit coupling, external magnetic fields, multi-dimensional exciton interactions in the spin-orbit coupled singlet states, and multi-dimensional exciton interactions in the triplet state are discussed.

I. Introduction

In order to describe the dynamics of exciton migration in the Frenkel limit,[1] it is not sufficient to consider only the time independent delocalized stationary states of a crystal. Because of the explicit localization introduced into the stationary states by phonon-exciton scattering, the electronic states, the phonon states, and phonon-exciton coupling must all be explicitly considered in terms of the crystal states.[2,3] Basically, the phonons introduce modulation of the intermolecular interaction which mixes the delocalized k states of the crystal and results in a state that can be described as a linear combination of the delocalized states.[4] In the Frenkel limit, this results in a partial localization of the electronic excitation but still allows for the excitation to propagate coherently as a wave packet provided the explicit linear combination of k states remains unchanged for times exceeding the time associated with the intermolecular exchange interaction. Indeed, it is the average frequency at which the linear combination of k states changes relative to the intermolecular interaction time that determines the primary mechanism responsible for electronic energy transfer in solids at both high and low temperatures. At low temperature the density of populated phonon states becomes sufficiently small that modulation of/or scattering between the exciton wave vector states k by the phonons is expected to be much less frequent than the effective intermolecular exchange time. It is important to note that in this limit the problem is not describable by the stationary Bloch solutions of the Schrodinger equations,[5]

$$\psi(p) = \frac{1}{\sqrt{n}} \sum_{r} e^{i\vec{p}\cdot\vec{r}/\hbar} u(r) \tag{1.1}$$

but rather by a superposition of Bloch states with a minimum spread Δp restricted by the wave packets uncertainty in position.

$$\Delta p \sim \hbar/\Delta r. \tag{1.2}$$

For the coherent limit to be meaningful the mean free path, ℓ, associated with excitons formed from a given superposition of Bloch states must be longer than the uncertainty of position, Δr, and hence longer than the lattice separation, $\vec{a}$. In such cases, a coherent Frenkel exciton can be viewed as a quasilocalized excitation propagating coherently as a wave packet at a velocity characteristic of both its energy and the linear combination of stationary crystal k states which describe the packet. This velocity is termed the group velocity and is given by

$$V_g(p) = (\partial\varepsilon/\partial p) \tag{1.3}$$

or

$$V_g(k) = \frac{1}{\hbar}\left(\frac{\partial\varepsilon(k)}{\partial k}\right). \tag{1.4}$$

For a one-dimensional crystal, in the nearest neighbor approximation the energy dispersion of the band,[6] $\varepsilon(k)$, is given by

$$\varepsilon(k) = E^{o} + 2\beta \cos ka \tag{1.5}$$

and is taken to be associated with translational equivalent interactions

along a direction $\vec{a}$. E^o is the electronic energy of the molecular excited state and β is the effective intermolecular interaction in the nearest neighbor approximation. $V_g(k)$ is then given by

$$V_g(k) = \frac{2\beta a}{\hbar} \sin ka. \tag{1.6}$$

The distance, $\ell(k)$, which an exciton propagates in a coherent fashion without changing its velocity is given by the lifetime of the coherent state, $\tau(k)$, times the group velocity of the wavepacket, i.e.,

$$\ell(k) = V_g(k) \cdot \tau(k); \tag{1.7}$$

$\ell(k)$ is thus equivalent to a mean-free path, and $\tau(k)$ in the stochastic approximation[7] corresponds to a lifetime or correlation time for the scattering of the wavepacket centered at k. <u>From a dynamical point of view, the important feature of coherent migration is that excitons can propagate in the crystal a variety of distances and at a variety of velocities depending upon the particular population distributions over the exciton and phonon bands and the exact nature of phonon-exciton coupling</u>.

In the one-dimensional limit, the group velocity is zero at the top and bottom of the band ($k = 0$ and $\pm\pi/a$) but $2\beta a/\hbar$ at the center of the band ($k = \pm\pi/2a$). Appreciable energy migration in one-dimensional crystals in the coherent limit requires a distribution over the non $k = 0$ and $\pm\pi/a$ states, preferably in the center of the band. The extent to which these and other k states contribute to the propagation of electronic energy is determined by the temperature, the exciton band width, and the form of

the distribution function. It is important to recognize that, in principle, non-Boltzmann distributions in the band can be established when the decay time of the electronic excited state to the ground state is shorter than the coherence time, $\tau(k)$. If, for example, only the $k = 0$ state is prepared, say via optical absorption from the ground state at low temperatures, and the excited state lifetime is shorter than phonon-exciton scattering to other k states, little exciton migration would be realized due to the stationary nature of the top and bottom of the band. When a thermal distribution characterizes the band, however, the number of excitons, $N(k)$, propagating with a velocity, $V_g(k)$, is given by the Boltzmann factor for the k state divided by the partition function[8] for the exciton band.

$$N(k) = \frac{D(k)\, e^{-E(k)/KT}}{\sum_k e^{-E(k)/KT}}. \tag{1.8}$$

One notes that very mobile states can be populated at reasonably low temperature provided the band dispersion is not too great.

The importance of coherent exciton migration is perhaps best illustrated by comparing it to the high temperature diffusion limited random walk process which is characterized by a density of populated phonon or localized vibrational states sufficient to limit the coherence lifetime of an exciton k state by inelastically scattering it to other states in the band. When this causes a change of k at a rate comparable to intermolecular energy exchange, wavepackets formed from the delocalized

Bloch functions of the crystal are no longer appropriate bases states for times exceeding $(\beta)^{-1}$ and the proper description of the exciton states is a unitary transformation of the k states to a set of orthogonal, k independent, localized Wannier functions.[9]

$$\phi(r) = \frac{1}{\sqrt{n}} \sum_{p} e^{-i\vec{p}\cdot\vec{r}/\hbar} \psi(p). \tag{1.9}$$

In this limit, the exciton migrates in a random walk manner through a resonant interaction between Wannier functions centered on adjacent lattice sites. The velocity of migration of the exciton is its RMS deviation per unit time from its starting position and is usually many orders of magnitude slower than coherent migration. For a molecular crystal with nearest neighbor molecules having an effective intermolecular interaction of 1 cm^{-1} and a lattice spacing, $\vec{a}$, of 4 Å, the random walk exciton velocity is 10^{-2} cm/sec while coherent states have a group velocity at the center of the band of 10^4 cm/sec. The mean-free path for random walk diffusion is 4 Å while states migrating coherently at the center of the band, for example, have a mean free path dependent upon $\tau(k)$ via

$$\ell(k = \pm\pi/2a) = \frac{2\beta a}{\hbar} \cdot \tau(k = \pm\pi/2a). \tag{1.10}$$

It is self-evident that the coherence length of the states in the center of the band can approach macroscopic dimensions if phonon-exciton scattering is weak (i.e., $\tau(k)$ is long) and the excited states are long-lived compared to $\tau(k)$. In principle, $\tau(k)$ could approach the lifetime of the excited

electronic state at very low temperatures where the distribution of phonon states approaches the $T \to 0$ limit. At intermediate temperatures where $\tau(k)$ is limited by phonon-exciton scattering an exciton initially at an energy $\varepsilon(k)$ scatters to other k' states at energies $\varepsilon(k')$ via phonon interactions in a time short compared to the excited electronic state lifetime but in a time long compared to intermolecular exchange. The net result is that the coherence time is shortened, the mean-free path or coherence length is attenuated, and the k states acquire an energy width $\Gamma(k)$, given by the reciprocal of the coherence lifetime of the individual k states, i.e.,

$$\Gamma(k) = \hbar[\tau(k)]^{-1}. \tag{1.11}$$

In effect, inelastic scattering of the excitons by the phonons introduces a time and temperature dependent damping of the wave packet states. For completeness, damping or localization of the stationary zeroth order states by other processes such as impurity or isotopic scattering can be incorporated into this description by expanding the delocalized unperturbed Bloch functions given by Equation 1.1 such that the coefficients in the expansion forming the perturbed wavefunctions satisfy difference equations associated with the perturbed periodic potential problem.[10-12] In such cases, the delocalized Bloch functions describing the pure crystal state are partially localized by impurity scattering and the impurity states themselves become significantly delocalized. Wave packet states can then be formed from a superposition of perturbed states resulting from

these scattering processes.

It is clear that in addition to the stationary states of the crystal a proper description of the dynamics of exciton migration must include (a) the group velocities of excitons, (b) the population distribution over the k states of the band, and (c) the coherence times for the individual k states and hence an explicit model for exciton scattering processes. This description views an exciton initially in a state characterized by an energy $\varepsilon(k)$ as scattering to a state at $\varepsilon(k')$ in a time on the order of the coherence lifetime but it allows for long range propagation via coherent migration in between scattering events.

In the first paper[8] in this series we described the importance of low temperature coherent exciton migration in providing a mechanism where by localized impurity states can be maintained in Boltzmann equilibria with the delocalized band states. The dynamics in this description were based on an ensemble average over the coherent wave packet group velocities at a fixed temperature and hence information about scattering in the individual wave packets was lost. In the following we present an experimental method and its associated theory based on electron spin resonance which allows one to investigate properties of the individual exciton wave packet states and their interactions with phonon states in the coherent limit. Although the development is made for triplet excitons in molecular solids application of the method and theory to other problems such as low temperature impuriton migration[13] is straightforward.

II. Electron Spin Resonance Absorption in Coherent Triplet Exciton States

From an experimental point of view, the above considerations require that careful attention be given to the relationship between the time associated with exciton migration and the correlation time of the particular experimental approach being employed. If, for example, the experimental correlation time is much shorter than $\tau(k)$ (as is the case for optical absorption), only manifestations of the coherent model are apparent from the data. Similarly, when the experimental correlation time is longer than $\tau(k)$ for all k, only the random walk processes are displayed. A measure of phenomena such as phonon-exciton scattering, $V_g(k)$, and $\ell(k)$ which are related to both coherent migration and diffusion limited migration can only be determined when the experimental correlation time is on the order of $\tau(k)$. It is on this basis that electron spin resonance[14,15] provides a direct probe into the dynamics of triplet excitons.

In the following electron spin resonance theory, the model adopted is a "one-dimensional" crystal in which only translationally equivalent intermolecular interactions along a single crystallographic direction have finite magnitudes. The excited triplet band is derived from intermolecular exchange coupling between the ground singlet and excited triplet states and is restricted to nearest neighbor interactions. In zero magnetic field the triplet band is split by electron spin dipolar repulsions into three parallel spin sublevel bands which will be designated as τ_x, τ_y, and τ_z. These correspond to states where the electron spins are correlated along the x, y, and z molecular axes, respectively. This is

illustrated in Figure 1a where the effective intermolecular exchange interaction is designated by β, and the energy of the molecular triplet state in the absence of intermolecular exchange by E^o. E^o is on the order of 30,000 cm^{-1} for aromatic molecules in their first excited triplet states. Zero-field splittings are typically tenths of wavenumbers[16] while triplet band dispersions, 4β, are on the order of tens of wavenumbers.[17] In the limit that no anisotropy of the zero-field splitting is introduced by intramolecular spin orbital coupling of the individual triplet spin sublevels to the singlet manifold, the band-to-band electron spin transition induced by a radiofrequency or microwave H_1 field (Cf. Figure 1a - ⇕) would be a homogeneously narrowed Lorentz line centered at the frequency characterized only by the spin dipolar parameters D and E. The line width is taken to be that associated with a "perfect crystal" spin-spin relaxation time T_2^p at 0°K.

A. The Effects of Group Velocity Dependent Relaxation Processes

Even when $\tau(k)$ is long compared to β^{-1} additional contributions to T_2 might be expected in the coherent limit when the temperature becomes finite. This could be particularly true for phenomena such as strong impurity scattering or other interactions capable of dephasing the rotating frame magnetization that depend upon <u>spacial</u> characteristics of the crystal. These might cause the spin ensemble to dephase at different rates depending upon which wave vector states were populated at any particular temperature. Crystal inhomogeneities or other phenomena that change the energy of the

zero-field splitting will be sampled faster by excitons in k states near the center of the band ($k = \pm\pi/2a$) than those at the top and bottom ($k = 0; \pm\pi/a$) because of the crystal volume sampled by the wave packet per unit time. Velocity dependence can be included in T_2 by associating with each wave packet state at energies $\varepsilon(k)$ a relaxation time $T_2(k)$. The total electron spin transverse relation time for a particular k state is then simply

$$\frac{1}{T_2^{\,k}} = \frac{1}{T_2^{\,P}} + \frac{1}{T_2(k)} \tag{2.1}$$

where $T_2(k)$ is weighted by the wave packet's group velocity $V_g(k)$; i.e.,

$$T_2(k) = C\left(\frac{2\beta a}{\hbar}\right) \sin\,(ka). \tag{2.2}$$

The constant C is taken to be proportional to the change, $\Delta\omega$, in the Larmor frequency per unit scattering event. Restricting $T_2(k) < \tau(k)$, the net result for a Boltzmann distribution of population across the triplet band is to produce a temperature dependent band-to-band transition which is the weighted sum of the individual Lorentz lines centered at ω_o each having a velocity weighted $T_2^{\,k}$. Letting

$$g^k(\omega) = \frac{T_2^{\,k}}{\pi}\left(\frac{1}{1 + (T_2^{\,k})^2(\omega - \omega_o)^2}\right) \tag{2.3}$$

be a single Lorentz line shape function[18] for one k state, the line shape function for a distribution over exciton states at a temperature T would be

$$G^T(\omega) = \sum_k N(k) g^k(\omega) \tag{2.4}$$

where N(k) is the number of excitons at energy $\varepsilon(k)$. For a thermal distribution,

$$G^T(\omega) = \sum_k \frac{T_2^{\,k}}{\pi} \left(\frac{D(k)\ e^{-\varepsilon(k)/KT}}{Z(T)} \right) \left(\frac{1}{1 + (T_2^{\,k})^2 (\omega - \omega_o)^2} \right) \tag{2.5}$$

where Z(T) is the partition function at temperature T and is given by

$$Z(T) = e^{-2\beta/KT} + \sum_{k \neq 0}^{\pm\pi/a} 2e^{-2\beta\cos(ka)/KT}, \tag{2.6}$$

D(k) is the degeneracy of the k state and $T_2^{\,k}$ is given by Equations 2.1 and 2.2. Substitution yields

$$G^T(\omega) = \frac{1}{\pi} \sum_k \left(\frac{D(k)\ e^{-2\beta\cos(ka)/KT}}{Z(T)} \right) \left(\frac{T_2^{\,P}}{\frac{2\beta a}{C\hbar}\, T_2^{\,P} \sin(ka) + 1} \right)$$

$$\cdot \left(\frac{1}{1 + \left(\frac{T_2^{\,P}}{\frac{2\beta a}{C\hbar}\, T_2^{\,P} \sin(ka) + 1} \right)^2 (\omega - \omega_o)^2} \right) \tag{2.7}$$

where $D(k) = 1$ if $k = 0$ and 2 otherwise.

Several important features which could allow this model to be verified experimentally emerge when the line shape function given by Equation 2.7 is examined in detail. Figure 2 illustrates the line shape profile, $G^T(\omega)$, for a band-to-band transition as a function of band width at a fixed temperature. The parameters $\Delta F(k = \pm\pi/2a)$ illustrated in the figures refer to the half width at half height of the band-to-band transition associated with the Lorentz component of k states in the center of the band having the largest group velocities $V_g(\pm\pi/2a)$, while $\Delta F(k = 0; \pm\pi/a)$ refers to the halfwidth at half height of the Lorentz component associated with the stationary states at $k = 0$ and $k = \pm\pi/a$. The latter is taken to be associated with T_2^p at the $T = 0°K$ limit. The transition has been arbitrarily centered at 3.000 GHz.

First, it can be seen from Figure 2 that to a large extent <u>the exciton partition function determines the overall line shape profile</u>. For Boltzmann distributions the population of a given set of k states depends upon the temperature to band width ratio; hence, as the band width increases from 1 to 8 cm^{-1} (Figure 2a-d), the contribution to the overall width of the transition from the very mobile k states near the center of the band decreases. This is reflected in the band-to-band transition as a pronounced narrowing with increasing band dispersion. This is also seen from the temperature dependence of the band-to-band transition as illustrated in Figures 3a and 3b. The overall effect of lowering the temperature is to narrow the electron spin transition by removing population from the

highly mobile states in the center of the band. The extent of the narrowing being proportional to $C(2\beta a/\hbar)$ depends implicitly upon the details of the incoherent events that cause the spins to dephase. This can be seen from a comparison of Figure 3a with 3b. In the latter, the amount which the spins dephase per incoherent scattering event is taken ten times that illustrated in Figure 3a and, thus, at all temperatures the transition appears significantly broader. Furthermore, there is a unique temperature dependence of the line shape profiles for any given dephasing rate $C(2\beta a/\hbar)$; hence, the band dispersion in principle can be determined experimentally.

Second, it is interesting to note that the number of wave vector states in the exciton band and consequently the number of molecules in a one-dimensional exciton chain also have a pronounced effect on the line shape. This can be particularly informative in highly doped mixed crystal systems.[19] A comparison of the line shapes in cases where the number of molecules in a chain have been taken as 1000 (Figure 3b) and 100 (Figure 3d) clearly demonstrates this feature. When the exciton band is characterized by a high density of states per unit energy (as is the case in Figure 3b), most of the width in the band-to-band transition comes from the less mobile k state near $k = 0$ or $\pm\pi/a$ because of the sharp peak in the one-dimensional exciton density of state function at the top and bottom of the band. However, when the number of k states is reduced by restricting the exciton chain length, the contribution of these less mobile states becomes proportionately smaller relative to the

states near the center of the band. Hence, the line shape profile acquires a broad baseline character (Cf. Figure 3d) from the extremely broad mobile states near the center of the band. Its sharp peak character, however, is from states near the bottom of the band. This is true only for systems in which both the number of states in the band is small and the change in $T_2(k)$ with k large. If the number of states in the exciton band is increased (i.e., the mixed crystal content or the impurity concentration is reduced) while the rest of the parameters of the system remain unchanged, a greater number of states with smaller group velocities contribute to the profile and a narrower line appears in place of the broad baseline. Although electron spin transitions in short exciton chains appear narrower in the peak portion of the lineshape, their overall width appears broader than the corresponding transition in longer exciton chains; however, the breadth appears near the baseline.

In the higher temperature limit when the coherence lifetime $\tau(k)$ becomes short and exciton migration is principally a random walk process, the k dependence of the velocity is lost and the exciton velocity is described by an RMS distance distribution per unit time. In this case, there should be no temperature dependence to the line width in one-dimensional systems. The line shape function is a simple Lorentz line characterized by some k independent effective T_2,[20,21] i.e.,

$$G(\omega) = \frac{T_2}{\pi}\left(\frac{1}{1 + T_2^{\,2}(\omega - \omega_o)^2}\right). \qquad (2.8)$$

It is important to recognize that the above description is only valid when spin orbit coupling is absent or identical for the spin sublevels. In such cases, there is no explicit k dependence in the Larmor frequencies, and thus, phonon-exciton scattering between k states does not broaden the electron-spin transitions by exchange averaging of different Larmor frequencies.

When the effects of selective spin-orbit coupling of singlet band with one or more of the individual spin sublevel bands are considered, however, an explicit k dependence is introduced into the triplet exciton zero-field splitting in the first Brillouin zone.[14,22] Basically, three different singlet states (or the magnetic sublevels of different triplet states) each with different band dispersions and energies couple in varying degrees selectively to the three triplet spin sublevel bands.[23] The net effect is to produce a shift in energy of the zero-field eigenstate via spin-orbit interactions. The shift is different, however, for each of the three spin sublevels. Moreover, since the triplet band dispersion is usually much less than that associated with the singlet band which is mixed into the triplet sublevel via spin-orbit interactions, there is a greater spin-orbit perturbation in the zero-field splitting at $k = 0$ or $k = \pm\pi/a$ depending upon the relative signs of the intermolecular interaction responsible for the band dispersions of the singlet and triplet, respectively. The importance of spin-orbit coupling cannot be underestimated, for it is precisely this which gives rise to a k dependence of the Larmor frequencies for the band-to-band electron spin transitions.

This is diagrammatically illustrated in Figure 1b. As has been shown by Francis and Harris[14] the resulting k dependence of the Larmor frequency, ω_o^k, reflect the band dispersion on a reduced scale and is given by

$$\omega_o^k = \omega_o + f4\beta \cos ka \tag{2.9}$$

where the reduction factor f is related to the details in the difference of spin-orbit coupling in the spin sublevel bands[14] and ω_o is the transition frequency in the center of the band. In such cases different Larmor frequencies can be associated with different k states, and the proper representation for electron spin resonance absorption in terms of the Bloch formalism[24] is a set of magnetic Bloch equations, one for each k state in the band, whose frequency components, ω_o^k, are coupled by phonon-exciton scattering.

B. Effects of Phonon-Exciton Scattering on Electron Spin Relaxation

In the rotating frame, the presence of a weak oscillating rf field of the form

$$\mathcal{H}(t) = -\gamma\vec{H}_1 \cdot \hat{S}_z \cos \omega t \tag{2.10}$$

connecting, for example, τ_x with τ_y spin sublevels via the electron spin operator $\hat{S}_z$ results in an in-phase, u, and out-of-phase, v, component of a complex moment, G_k, given by[25]

$$G_k = u_k + iv_k. \tag{2.11}$$

Representing ω as the applied microwave frequency and ω_o^k as the resonant microwave frequency associated with the spin sublevels of the kth state in the band, the complex moments obey the following Bloch equations (one equation for each k state in the exciton band).

$$\frac{dG_k}{dt} + \left[\frac{1}{T_2(k)} - i(\omega_o^k - \omega)\right]G_k = -i\gamma H_1 M_o^k. \tag{2.12}$$

M_o^k should be related to the exciton density of states function and the particular form of distribution function characterizing the population in the exciton band. For a Boltzmann distribution

$$M_o^k = \frac{D(k)[P_m e^{-E^m(k)/KT} - P_n e^{-\varepsilon^n(k)/KT}]}{Z(T)} \tag{2.13}$$

where P_m and P_n are the populations of the mth and nth spin sublevels which are being coupled by the microwave field and Z(T) is the partition function for the triplet exciton bands. Since selective spin orbit coupling results in only very small differences in the dispersions of the individual sublevel bands, the exponential factors in Equation 2.13 are effectively equal. Thus, to a high degree of accuracy Equation 2.13 can be rewritten as

$$M_o^k = \frac{C_{mn} \cdot D(k)e^{-\varepsilon(k)/KT}}{Z(T)} \tag{2.14}$$

where C_{mn} is the difference in populations of the mth and nth spin sub-levels. $\varepsilon(k)$ and $Z(T)$ are given by Equations 1.5 and 2.6, respectively. It is important to note that spin alignment[26] in the laboratory frame is equivalent to magnetization in the rotating frame,[27] and thus, Equation 2.12 is valid in zero-field even though no magnetization exists in the laboratory frame. It will be assumed that $T_2(k)$'s are homogeneous. The weak field modified Bloch equations are

$$\frac{dG_k}{dt} + (1/T_2(k))G_k - i(\omega_o{}^k - \omega)G_k = -i\gamma H_1 \frac{D(k)e^{-\varepsilon(k)/KT} \cdot C_{mn}}{Z(T)}. \quad (2.15)$$

There are N linear equations corresponding to the N molecules making up a single linear exciton chain.

The effects of phonon-exciton scattering in the chain can be incorporated into these equations through a scattering matrix which completely spans the basis states of the Frenkel excitons. Let $(\tau_{kk'})^{-1}$ represent the probability per unit time for scattering of an exciton initially in a state having energy $\varepsilon(k)$ to a final state having an energy $\varepsilon(k')$, each state having associated with it a Larmor frequency $\omega_o{}^k$ and $\omega_o{}^{k'}$, respectively. Furthermore, assume that spin-phonon coupling is negligible, which implies that phonon-exciton scattering is spin independent. Under these conditions the N modified Bloch equations are written as

$$dG_k/dt + (1/T_2(k))G_k - i(\omega_o{}^k - \omega)G_k = -i\gamma H_1 \frac{D(k)e^{-\varepsilon(k)/KT} \cdot C_{mn}}{Z(T)}$$

$$+ \sum_{k'} G_{k'}/\tau_{k'k} - G_k/\tau_{kk'}. \quad (2.16)$$

The form of Equation 2.16, however, places several restrictions on the effect of phonon-exciton scattering. It assumes that the averaging of the Larmor components ω_o^k via phonon-exciton scattering is a stochastic Markoffian[7,28] process and thus (a) the time for the actual scattering process from k to k' is much shorter than the lifetime of a particular k state; (b) the difference in energy between the initial and final exciton k states in a scattering event is larger than the energy associated with the uncertainty width of the individual k states; and finally, (c) there is no spin memory between the Larmor components ω_o^k and $\omega_o^{k'}$ corresponding to scattering from the exciton states k to k' via phonon interactions. With these restrictions in mind we display $(\tau_{kk'})^{-1}$ or the probability per unit time for an exciton being scattered by a phonon from k to k' as a "golden rule" rate[29]

$$(\tau_{kk'})^{-1} = \rho_\varepsilon(k') \sum_{\lambda,q,q'} \rho_p(q')\left(\frac{1}{\exp(E^\lambda(q)/KT) - 1}\right) \cdot$$

$$|\langle kq|H_{ep}^\lambda|k'q'\rangle|^2 \delta(k + q, k' + q'). \qquad (2.17)$$

$\rho_e(k')$ and $\rho_p(q')$ are the exciton (subscript e) and phonon (subscript p) density of states functions evaluated at the energy of the wave vector k' and q', respectively. λ is the index which runs over the phonon branches and $E^\lambda(q)$ is the energy of the qth wave vector of the λ phonon branch. The sum over phonon states q and q' is restricted to scattering events that conserve both the total energy and momentum of the initial and final exciton-phonon states $\langle kq|$ and $\langle k'q'|$ and H_{ep}^λ is the exciton-phonon coupling

Hamiltonian. In weak oscillating rf fields and steady state

$$dG_k/dt = 0 \tag{2.18}$$

and the electron spin resonance line shape function, $G(\omega)$, is given by the sum over k of the imaginary components of the complex moment, G_k, i.e.,

$$G(\omega) = \mathrm{Im} \sum_k G_k. \tag{2.19}$$

The importance of Equations 2.16 through 2.19 cannot be underestimated for they provide in principle a direct means of obtaining from experiment both qualitative and quantitative information on the mechanism of triplet exciton migration in the coherent limit, the random walk limit and, in fact, in the region intermediate between the two. Although the latter requires the unwieldy solution of many simultaneous equations, the two extreme limits can be readily solved.[30]

The first will be termed the <u>strong scattering case</u> and occurs when $(\omega_o^k - \omega_o^{k'})\tau_{kk'} << 1$ and corresponds to the random walk limit. In effect, phonon-exciton scattering results in a rate of change of the exciton states $(k \rightarrow k')$ fast compared to the differences in the corresponding Larmor frequencies $(\omega_o^k - \omega_o^{k'})$; thus, the effective electron spin transition frequency becomes the average of ω_o^k and $\omega_o^{k'}$. If for all k, $(\omega_o^k - \omega_o^{k'})\tau_{kk'} << 1$, the band-to-band transition will appear as a homogeneously narrowed line centered at some weighted average of all the frequencies. This is expected at high temperatures and is essentially the same as

derived and expanded upon by McConnell and co-workers[31] from a different approach.

The second or <u>weak scattering case</u> results when $(\omega_o^k - \omega_o^{k'})\tau_{kk'} >> 1$. This corresponds to the limit in which phonon-exciton scattering causes the linear combination of triplet exciton states to change on a time $(\tau_{kk'})$ slow compared to the differences in the Larmor frequencies $(\omega_o^k - \omega_o^{k'})$. In such cases the coherent nature of the individual k states of the triplet band can be sampled by the rf field, and the spin resonance line shape becomes the sum of the individual transitions at ω_o^k each having a width corresponding to an effective $T_2(k)$ given in Equation 2.15 and each weighted by the population distribution, N(k), evaluated at an energy $\varepsilon(k)$. It should be noted, however, that in this limit, the width of each Lorentz line centered at ω_o^k includes a lifetime broadening term introduced by inelastic phonon-exciton scattering through Equation 2.16. Hence, $T_2(k)$ is given by

$$T_2(k)^{-1} = (T_2^p)^{-1} + (\tau(k))^{-1} \qquad (2.20)$$

where T_2^p represents the homogeneous relaxation time at zero degrees Kelvin. The relationship between phonon-exciton scattering and the lifetime of a k state is given simply by the sum over all decay channels or the individual scattering rates $\tau_{kk'}$; i.e.,

$$\tau(k)^{-1} = \sum_{k'} (\tau_{kk'})^{-1}. \qquad (2.21)$$

Consequently, specific features of phonon-exciton scattering can be discerned from the electron spin band-to-band transitions line shape

function since the Lorentz line width at each ω_o^k is given essentially by $\tau(k)^{-1}$ when phonon-exciton scattering rates exceed $(T_2^p)^{-1}$. This point can be better illustrated by considering models for phonon-exciton scattering in various limits. We will restrict the discussion, however, to cases where the population of the band states is characterized by a Boltzmann distribution function. In these cases the intensity of the band-to-band transitions evaluated at ω_o^k are weighted by M_o^k given by Equation 2.14.

1. Phonon-Exciton Scattering in the Narrow Band Coherent Limit

The first case in the weak scattering limit we will consider is when the exciton dispersion is narrow compared with the dispersion of the phonon branches populated at any particular temperature. Restricting the discussion to very low temperatures (1-10°K) where the primary limitation on the coherence time will be exciton scattering with the acoustic phonons[32] (the population of higher energy phonons being very small), the individual scattering rates $\tau_{kk'}^{-1}$ can be displayed in an extremely simple form when the scattering events are limited to events in which a phonon with wave vector q and an exciton with wave vector k interact to produce final states which are single phonon and single exciton states having wave vectors q' and k', respectively. Naturally, such scattering events must simultaneously conserve both the total momentum and energy of the initial and final states. That is,

$$\hbar k + \hbar q = \hbar k' + \hbar q' \qquad (2.22)$$

and

$$E(k) + E(q) = E(k') + E(q') \tag{2.23}$$

must be satisfied. Consider first the region of the acoustic phonon dispersion that is near linear in energy[33] as illustrated in Figure 4a. When the dispersion of this portion of the acoustic band is large relative to the exciton band, the phonon group velocities are many times those of even the most mobile exciton states. In order to conserve both momentum and energy in the scattering process, the derivative of $\varepsilon(k)$ with respect to initial state k must be the same as the derivative of E(q) with respect to the phonon wavevector q for all energies $\varepsilon(k)$ at which scattering occurs, i.e.,

$$\frac{\partial \varepsilon(k)}{\partial k} = \frac{\partial E(q)}{\partial q}. \tag{2.24}$$

The left and right sides of Equation 2.24 are simply the exciton and phonon group velocities multiplied by $\hbar$, respectively. When there are large differences in the phonon and exciton dispersions, this condition cannot be easily satisfied, and it is only in the limit of Δk and $\Delta q \to 0$ that scattering can conserve both momentum and energy between initial and final states. Such is the case for acoustic phonons in the linear region of their dispersion. However, when the phonon dispersion becomes non-linear, the group velocities of some phonon states can match the group velocities of the exciton states, and both the total energy and momentum

can be conserved between initial states $\langle kq|$ and final states $\langle k'q'|$. Adopting the hypothesis that phonon-exciton scattering shortens the coherence lifetime of an exciton k state only when the group velocities of the excitons and phonons are approximately equal, Equation 2.17 is greatly simplified. In such cases, the scattering rates, $(\tau_{kk'})^{-1}$, are simply proportional to the number of phonons populating the q^kth phonon state, whose group velocity matches the group velocity of the exciton state k, times the density of final exciton and phonon states. The number of phonons, however, is given by the Planck distribution; hence,

$$(\tau_{kk'})^{-1} = \rho(q')\rho(k') \frac{1}{\exp(E^{\lambda}(q^k)/KT) - 1} |\langle kq|H^{\lambda}_{ep}|k'q'\rangle|^2. \quad (2.25)$$

It should be noted that the rate of scattering excitons by phonons in the non-linear region is enhanced by the fact that it occurs between phonon states q and q' whose density of states functions, $\rho(q)$ and $\rho(q')$, are large. When the exciton band dispersion becomes much less than the acoustic band dispersion, the variation in the range of states capable of scattering with k states becomes progressively more restricted to fewer q and q' states, and therefore the difference between $\rho(q')$ and $\rho(q)$ becomes smaller. Furthermore, since $\rho(k')$ approaches a k independent constant in the zero exciton band dispersion limit, the scattering rates $(\tau_{kk'})^{-1}$ must become uniform in the narrow exciton band limits, at which point the exciton k state coherence lifetimes $\tau(k)$'s would become equal for all k. The temperature dependence of $\tau(k)$ becomes simply the Planck distribution function[34]

evaluated at the energy of the acoustic phonon state that has the lowest group velocity. Denoting the energy of this state as $E^{\lambda}(q^{k})$, the exciton's coherence time is given by

$$\tau(k)^{-1} = (\tau^{*})^{-1}(\exp(E^{\lambda}(q^{k})/kT) - 1)^{-1} \tag{2.26}$$

where $(\tau^{*})^{-1}$ is an effective scattering time given by the temperature independent term

$$(\tau^{*})^{-1} = \rho(q') \sum_{k'} \rho(k') |\langle kq|H^{\lambda}_{eq}|k'q'\rangle|^{2}. \tag{2.27}$$

The summation over k' is restricted to the interval, around the initial k value, in which the phonon and exciton group velocities match. This interval is narrow in the narrow exciton band limit, and therefore an exciton can only scatter to states whose k values and group velocities do not differ greatly from that of the initial state. Thus, scattering may not greatly impede the long range migration of excitons. When $T \ll E^{\lambda}(q^{k})$, as is usually the case at temperatures below the Debye temperature,[35] $\tau(k)$ is given by

$$\tau(k)^{-1} \simeq (\tau^{*})^{-1} \exp(-E^{\lambda}(q^{k})/kT) \tag{2.28}$$

and hence <u>the excitons coherence time vs. temperature appears as a k independent exponentially decreasing function with increasing temperature</u>:

$$\tau(T)^{-1} \equiv \tau(k)^{-1}. \tag{2.29}$$

The principal manifestation of the electron spin band-to-band transition in this narrow band limit at a given temperature is to give all frequency components, ω_o^k, the same effective widths. Thus, the line shape function represents the sum over N independent Lorentzian absorption curves, each centered at ω_o^k with a line width related to $\tau(k)$ at a temperature T. In zero magnetic field the area under each transition is proportional to the probability at a given temperature that the exciton k state is populated. For a Boltzmann distribution across the exciton band, the lineshape function is given by

$$G^T(\omega) = \sum_k \frac{D(k)e^{-2\beta\cos ka/KT}}{Z(T)} \cdot \frac{T_2(T)}{\pi} \frac{}{[1 + (T_2)^2(\omega - \omega_k^o)^2]} \qquad (2.30)$$

where

$$\frac{1}{T_2(T)} = \frac{1}{T_2^p} + \frac{1}{\tau(k)} \qquad (2.31)$$

and ω_k^o, given above, is different for each k state. Since $G^T(\omega)$ is normalized by the one-dimensional exciton partition function Z(T), line shapes at various temperatures may be compared. Provided that either T_2^p is known or $1/T_2^p < 1/\tau(T)$, the functional dependence of $T_2(T)$ with temperature provides an experimental test of this limit. $G^T(\omega)$ is similar to the line shape function arrived at by Francis and Harris[14] from phenomenological point of view valid at a single temperature in the limit that the number of k states in the exciton band is large.

The general features of the line shape theory in the coherent narrow band limit are illustrated in Figures 5 and 6. In all cases, we have chosen 20 cm^{-1} for $E^{\lambda}(q^k)$, the energy of the acoustic phonons having the slowest group velocity, which is a reasonable value for molecular crystals.[36] Additional parameters in Equations 2.28 and 2.31 were set as follows

$$T_2^{\,p} = 10^{-6} \text{ sec}$$
$$\tau^* = 8.9 \times 10^{-10} \text{ sec.}$$

Finally, the difference in the Larmor frequencies between $\omega_o^{\,k}$ $(k = 0)$ and $\omega_o^{\,k}$ $(k = \pm\pi/a)$ due to selective spin orbit coupling has been taken as 20 MHz, a value near that experimentally found[22] in 1,2,4,5-tetrachlorobenzene for the D - |E| band-to-band transition. In Figure 5 the band-to-band transitions have been calculated using Equation 2.30 for a series of band widths, 4β. All transitions are calculated for $T = 4.1°K$. Several features are important. First, the ratios of the peak heights near $(k = 0)$ and $(k = \pm\pi/a)$ are related to a Boltzmann distribution weighted density of states maxima[37] at $k = 0$ and $k = \pm\pi/a$. Hence, if $T_2(T)$ is measured or known, the band dispersion immediately follows from the ratio of the transition intensity at $k = 0$ vs. $k = \pm\pi/a$. Second, the width of any packet of k states which can be prepared by the microwave field is proportional to $(T_2(T))^{-1}$; hence, selective k dependent population changes between the magnetic spin sublevels can be produced by microwave pulses at the appropriate frequency. This allows other k-dependent phenomena

such as bimolecular exciton anihilation,[38] exciton-trapping,[39] etc., to be experimentally investigated in the coherent limit. Third, when $T_2^p << \tau(k)$, $T_2(T)$ is the coherence lifetime of the wave vector states having velocities, $V_g(k)$; hence, the k dependence of the mean-free-path, $\ell(k)$, follows from

$$\ell(k) = V_g(k) \cdot T_2(T). \tag{2.32}$$

In Figure 6 the exciton band-to-band transition has been calculated using Equation 2.30 for several bandwidths 4β and for various temperatures given the above values for the parameters $E^\lambda(q^k)$, T_2^p, and τ^*. The lowest temperature used in the calculation, 3.1°K, was chosen such that the contribution to $T_2(T)$ from T_2^p and from phonon exciton scattering $\tau(T)$ are equal. At this temperature, broadening of the transition due to exciton-phonon scattering is beginning to become significant. At 4.1°K, the population of phonons having energy $E^\lambda(q^k)$ is greatly increased and $\tau(T)$ becomes the major contribution to $T_2(T)$. This results in further broadening of the transition and a shift in frequency of the band-to-band transition maxima. As the transition becomes increasingly broad, the use of the ratio of the intensities of the maxima to determine the exciton band width without explicitly considering $T_2(T)$ becomes an increasingly less valid approximation. By 5.1°K the contribution to $T_2(T)$ from exciton-phonon scattering has broadened the individual k state transitions to the extent that the exciton band-to-band transition has lost its two peak structure, and the system is becoming progressively farther removed from the weak scattering limit, $(\omega_o^k - \omega_o^{k'})\tau_{kk'} < 1$.

It is important to note, however, that the effects of elastic scattering or damping which can result in a significant reduction in $\ell(k)$ are not manifest in the above theory. This is because physical phenomena that localize the band by simply mixing + with - k states are not detectable by the broadening of the band-to-band electron spin transition because of the equality of the Larmor frequencies ω_o^k and ω_o^{-k}. $\ell(k)$ given above can only be regarded as the mean distance between inelastic scattering events. Other experiments, such as the dynamics of exciton trapping,[8] are necessary to establish $\ell(k)$ in the presence of phenomena such as isotopic or impurity localization.[10-13]

Finally, the effects of an oriented magnetic field on the line shape in the narrow band coherent limit can be anticipated from behavior of the spin Hamiltonian with a magnetic field. At each value of the wave vector k, the zero-field spin Hamiltonian consists of a k independent spin-spin term and a k dependent spin-orbit term, and consequently, the zero-field eigenvalues are different for different values of k. A Zeeman perturbation will result in a shift of ω_o^k relative to $\omega_o^{k'}$ that under certain circumstances gives rise to a field-dependent $(\omega_o^k - \omega_o^{k'})$ difference for the three electron spin band-to-band transitions. A difference $(\omega_o^k(k=0) - \omega_o^{k'}(k'=\pm\pi/a))$ for two or more of the zero-field band-to-band transitions is sufficient to ensure that the $(\omega_o^k - \omega_o^{k'})$'s are field-dependent for all k and k'. Selective spin-orbit coupling of the spin sublevels with excited singlet states provides the necessary differences in the Brilloin zone boundary electron spin band-to-band transition frequencies. The

effect of a magnetic field is simply to change the overall spin orbit induced width of the zero-field band-to-band transitions and shift the center frequency $\omega_o^k (k=\pm\pi/2a)$ to a new value determined by both the zero-field and Zeeman Hamiltonians. In the weak phonon-exciton scattering limit, the line shape should remain essentially unchanged with field except for a different overall width. In the intermediate scattering region, however, the $(\omega_o^k - \omega_o^{k'})\tau_{kk'}$'s are on the order of unity. Since $(\omega_o^k - \omega_o^{k'})$ is field-dependent, it is expected that at certain fixed temperatures the band-to-band electron spin transitions can be obtained both in the weak and strong scattering cases by varying the magnitude of the applied field and thereby effecting a change in $(\omega_o^k - \omega_o^{k'})$ without affecting the phonon-exciton scattering probabilities $(\tau_{kk'})^{-1}$. Thus, in principle, one can experimentally sample the phonon-exciton correlation time without changing phonon-exciton scattering <u>per se</u>. It is expected, given enough experimental data, that only one set of scattering parameters, $\tau_{kk'}$, and hence a single model for phonon-exciton scattering would be capable of fitting all the data at a fixed temperature.

2. Effects of Phonon-Exciton Scattering in the Intermediate Band Width Region

The second region of interest is where the acoustic phonon dispersion is approximately the same in its linear region as the exciton dispersion. The salient difference between this region and the narrow band region is that there are always acoustic phonons in the linear region which can

scatter with certain exciton states and simultaneously conserve the total momentum and energy in the overall process. If, for example, the group velocity of the exciton states in the center of the band match the group velocity of the compression wave associated with acoustic phonons in the linear region, $\tau(k)$ would be severely attenuated for exciton states in the center of the band ($\sim k = \pm\pi/2a$), while in the top and bottom of the band would show characteristics similar to the narrow band case. It is important to note that the most mobile exciton states in this case suffer the greatest phonon scattering and consequently have the shortest $\tau(k)$. From the point of view of energy migration approaching macroscopic dimensions, at first sight this case may seem unfavorable. Such is not the case, however, because the slopes of the exciton and phonon dispersions will only match over a small region of k space; hence, an exciton initially having quantum number k can only scatter to a final state k' which is in the small region around k where the slopes of the dispersions match. An exciton traveling with some initial velocity $\vec{V}_g(k)$ will scatter to a new state with almost the same velocity, $\vec{V}_g(k')$. Thus, phonon scattering of coherent excitons at reasonably low temperatures will not greatly impede the exciton's migration although it will average the Larmor frequencies of the k states involved in the scattering. (The conservation of k does not apply to impurity scattering of the excitons since k will no longer be a good quantum number due to the rapid variation of potential near the impurity.)

The band-to-band electron spin resonance transitions could appear very unusual depending upon the strength of the resonant scattering in

the center of the band. If it is sufficient to result in the strong scattering limit, $(\omega_o^{\ k} - \omega_o^{\ k'})\tau_{kk'} < 1$ for k and k' states near $\pm\pi/2a$, then those spin transitions would appear exchange narrowed while the transitions at the top and bottom of the band would remain in the weak scattering non-exchange limit, $(\omega_o^{\ k} - \omega_o^{\ k'})\tau_{kk'} > 1$. The net effect is for the band-to-band transition to have an exchange narrowed T_2 near ω_o $(k \sim \pm\pi/2a)$ and a non-exchange narrowed longer T_2 at ω_o $(k \sim 0;\pm\pi/a)$ with intermediate distributions of T_2's at values between the $k = 0$ and $k = \pm\pi/a$ wavevector states. As the temperature is raised two features would be apparent. First, the outsides of the band-to-band transitions would broaden and diminish in intensity relative to the transitions at ω_o $(k \sim \pm\pi/2a)$. Further increasing the temperature would cause the center ω_o $(k \sim \pm\pi/2a)$ region to broaden slightly via increased phonon-exciton scattering with increased temperature. When phonon-exciton scattering became sufficiently strong, the central region would narrow and the ω_o $(k \sim 0;\pi/a)$ transition would completely disappear by virtue of the strong scattering limitation,

$$(\omega_o^{\ k} - \omega_o^{\ k'})\tau_{kk'} < 1 \qquad (2.33)$$

being achieved for all k states. The important qualitative point about this region is that the exciton states should show a pronounced k dependence in the scattering which can result in the strong scattering limit at the center of the band at much lower temperatures than would be required to have k states at the top and bottom of the band in the strong scattering limit.

3. Effect of Phonon-Exciton Scattering in the Broad-Band Coherent Limit

A third case of interest is when the triplet exciton dispersion becomes greater than the acoustic phonon dispersion. In such cases, in a one-dimensional model, there will always be a region of exciton wave vectors which will have the same group velocity as the acoustic phonons in their linear region. Accordingly, strong resonant scattering is expected. However, as illustrated in Figure 4c, the wavevector states of the exciton band that are scattered in this limit are in the proximity of $k = 0$ and $\pm\pi/a$, and consequently, only the relatively immobile excitons, say k', suffer a short coherence time $\tau(k')$. In this limit, the highly mobile exciton states in the center of the band should only be weakly scattered. Furthermore, because only slower phonon states become populated in the nonlinear region, increasing temperature should not result in an appreciable increase in phonon-exciton scattering in the center of the band. States near the top and bottom of the band, however, will be progressively more strongly scattered with increasing temperature. Extension of our scattering model to these states is straightforward. $\tau(k')$ for exciton states which have group velocities equal to the group velocities of the scattered phonons is simply proportional to the total number of these phonons available at a given temperature. Using the Planck distribution function[34] for the number of acoustic phonons, q, at energies $E(q)$ for which $V_g(q) = V_g(k')$, $\tau(k')$, is given by

$$\tau(k') \sim \sum_q \left(\frac{1}{\exp(E(q)/kT) - 1} \right) \qquad (2.34)$$

It is important to stress that the k dependence in Equation 2.34 is restricted to only those few exciton states whose group velocities match the phonon group velocity over some energy span given by the sum over q. Figure 7 illustrates the dependence of the coherence time of these states as a function of temperature. The values for curves labeled 1.25, 2.5, 5, 10 and 15 cm^{-1} correspond to the scattering events that span the indicated energy increment of the phonon dispersion. For example, the curve labeled 5 cm^{-1} is $\tau(k')$'s for phonon-exciton scattering in which the exciton group velocity $V_g(k)$ equals phonon group velocities from phonon energies zero to 5 cm^{-1} along linear region of the phonon dispersion. One notes that the functionality of $\tau(k')$ is given principally by the Boltzmann factor and is moderately insensitive to the extent to which the group velocities match. Moreover, $\tau(k)$, to a first approximation, is almost linear with temperature, particularly when $kT > E(q)$.

The important qualitative point is that when the exciton dispersion is greater than the acoustic dispersion $\tau(k)$ should be constant in the center of the band at all temperatures. Hence, long range energy migration in the coherent limit is greatly favored providing the temperature is sufficient to populate states near $k = \pm\pi/2a$ to a significant extent but low enough to allow coherent migration. Obviously, one wants a crystal where the phonon dispersion is extremely small and where the triplet band is narrow. Ideally one would like the acoustic phonon dispersion, $\Delta\rho$, to be on the order of kT but less than the exciton band width. Whether or not this can be realized for low lying triplet bands is highly speculative.

The manifestations of this limit on the electron spin band-to-band transition are clearly indicative of the model. Strong resonant scattering with k states near the top and bottom of the exciton band could result in the strong-scattering condition.

$$(\omega_o^{\ k} - \omega_o^{\ k'})\tau_{kk'} < 1 \tag{2.35}$$

to be satisfied while most k states in the center of the band could be in the weak scattering limit. Consequently, the effective T_2 at $k \sim \pm\pi/2a$ would be long while T_2 would be short at the values of k near k = 0 and $\pm\pi/a$. As the temperature is raised, exchange narrowing of the k state microwave transitions near 0 and $\pm\pi/a$ would be expected; consequently, the wings of the exciton esr line would become progressively sharper while the region at the center of the band would remain broad.

In summary, one notes that the effects of phonon-exciton scattering on the electron spin band-to-band transition in the coherent limit show distinct qualitative and quantitative differences in the line shape functions in both the narrow band and broad band limit and in the region intermediate between the two. Next, we consider additional interactions which are static in nature but which also affect the appearance of the electron spin band-to-band electron spin resonance transition.

C. K Dependent Broadening via Two-Dimensional Translational Equivalent and Non-Equivalent Interactions

Up to now we have only considered explicitly the spin resonance of excitons associated with nearest neighbor one-dimensional translational

equivalent interactions. When two-dimensional bands are considered we must clearly delineate precisely which features we wish to treat.

1. Effects of Two-Dimensional Dispersion in the Singlet Band

To begin with, we consider the case where the triplet band extends over two dimensions both being associated with translational equivalent interactions. Furthermore, let there be a nearest neighbor intermolecular exchange interaction, β, principally along one of the two directions, say $\bar{a}$. In the absence of spin orbit coupling the triplet band dispersion, in such cases, appears as three parallel "ribbons" each ribbon being split from the other by spin dipolar repulsions. The coordinates are taken to be associated with wave vectors along the two translationally equivalent directions. If the singlet band that is mixed with a specific triplet spin sublevel band via spin orbit interactions has dispersion in both directions $\bar{a}$ and $\bar{b}$, then the energy separation between the singlet and triplet bands is dependent upon the singlet wave vectors, k_a and k_b. The net result of two-dimensional dispersion in the singlet band is to introduce a k_a and k_b dependence into the zero-field splitting of the triplet spin sublevel bands via intramolecular spin orbit coupling. Hence, a single microwave frequency ω_o will generally connect spin sublevels at two points on the triplet band surface, one at $k_a k_b$ and the other at $k_{a'} k_{b'}$. The only exception in this twofold k dependence is for Larmor frequencies corresponding to the maximum and minimum energy separation between the two triplet bands. These points have associated with them

only one ω_o^k. Naturally this approach can be extended to three dimensions with the corresponding increased functional convolution of ω_o on the k states. As far as the microwave transitions are concerned, there are several complexities which arise but as we shall see, they are fairly easy to deal with under most circumstances.

The principle effect of two-dimensional band dispersion in the singlet states and one-dimensional band dispersion in the triplet state is to have associated with the ω_o's two contributions to the Lorentz line widths, one from $\tau(k_a k_b)$ and the other from $\tau(k_a, k_b,)$. It is expected, however, that these coherence times will be virtually identical because the small energy shift from spin-orbit coupling along $\vec{b}$ is hardly enough to provide a change in the phonon-exciton scattering rates along $\vec{a}$. In other words, $\tau_{k_a k_b}$ are the same for a given k_a regardless of the value of k_b. A further complication arises, however, from two-dimensional singlet dispersion that directly affects the ω_o dependence of states possessing a given group velocity, $\nu_G(k)$. This can be illustrated by the following cases. Consider first, the effects of spin orbit coupling contributions to the zero-field splitting when the singlet dispersion along $\vec{b}$ is much greater than along $\vec{a}$ ($\Delta_b^{singlet} > \Delta_a^{singlet}$); further suppose for the point of illustration that the singlet and triplet band widths are identical. Under these circumstances there would be no anisotropy in the zero-field splitting along $\vec{a}$ but only along $\vec{b}$. Since the triplet band dispersion along $\vec{b}$ is taken to be zero, the group velocities $V_g(k)$ along b would all be the same (excluding the extremely small perturbation due to S.O. coupling);

hence, $\rho(k)$ along $\vec{b}$ is a constant. The line shape function under these circumstances would essentially be k independent, and is given by

$$I(\omega) = \zeta_{\omega}^{b} \int_{a} \rho(\varepsilon_a) \exp(-\varepsilon(k_a)/KT) d\varepsilon_a \qquad (2.36)$$

where ζ_{ω}^{b} is the k_b dependent S.O. coupling perturbation to the zero-field splitting along $\vec{b}$. We see that depending upon the magnitude of contributions to the line shape from examples approaching the above limit, the observed band-to-band transition can be broadened by an entirely static effect which is independent of phonon-exciton scattering.

Next consider the case where $\Delta_a^{singlet} > \Delta_b^{singlet}$. In this case, the principal k_a dependence of ω_o is retained and as before there are points $k_a k_b$ and $k_{a'} k_{b'}$ of equal zero-field splitting and a single ω_o having associated with it two $\tau(k)$'s, $\tau(k_a k_b)$ and $\tau(k_{a'} k_{b'})$. However, the points $k_a k_b$ and $k_{a'} k_{b'}$ can correspond to quite different regions in the triplet band. In particular, they can have considerably different group velocities. Therefore, $\tau(k_a k_b)$ and $\tau(k_{a'} k_{b'})$ might be significantly different in this case. The effective width associated with $\omega_o(k)$ is related to

$$\tau(k)^{-1} = \tau(k_a k_b)^{-1} + \tau(k_{a'} k_{b'})^{-1} \qquad (2.37)$$

and consequently the transition at $\omega_o(k)$ appears to be homogeneously broadened by phonon-exciton scattering at two points in the Brillouin zone. This is not a serious limitation on the interpretation of the observed line width, since it cannot average Larmor components in a significantly different manner than what has already been described. The principle qualitative features of the transitions are maintained. Only the quantitative evaluation of $\tau(k)$ will be in error. $\tau(k)$ could appear experimentally

shorter than it is in reality. From the interpretation of the electron spin resonance lineshape function, one errors on the side of less coherence, not more.

2. Effects of Two-Dimensional Dispersion in the Triplet Band

When an additional intermolecular exchange interaction associated with the translationally equivalent direction $\vec{b}$ in the triplet band acquires a significant value, (the largest being along $\vec{a}$) the separations between any two of the three triplet spin sublevel bands in zeroth order are equal at all values of $k_a k_b$ and $k_{a'} k_{b'}$. The electronic energy of spin sublevel surfaces, however, varies in both directions $\vec{a}$ and $\vec{b}$. As an example, consider the case where the band dispersion along $\vec{a}$, $4\beta^a$ is larger than along $\vec{b}$, $4\beta^b$, $\beta^a > \beta^b$. In such a case, when a Boltzmann distribution describes the populations the largest population is to be found at $k_a, k_b = (0,0)$ for a negative dispersion along both directions. The smallest populations are to be found at the four points on the first Brillouin zone boundary $k_a, k_b = (\pm\pi/a, \pm\pi/b)$. The general form of the Boltzmann population distribution for all k_a, k_b is given in the nearest neighbor approximation by the two-dimensional function $N(k_a, k_b)$ where

$$N(k_a,k_b) = \frac{D(k_a,k_b)e^{-(\varepsilon(k_a)+\varepsilon(k_b)/KT}}{\sum_{k_a}\sum_{k_b} D(k_a,k_b)e^{-(\varepsilon(k_a)+\varepsilon(k_b))/KT}} \qquad (2.38)$$

$\varepsilon(k_a)$ and $\varepsilon(k_b)$ are given by

$$\varepsilon(k_a) = 2\beta_a \cos(k_a \bar{a}) \tag{2.39}$$

and

$$\varepsilon(k_b) = 2\beta_b \cos(k_b \bar{b}) \tag{2.40}$$

Selective spin orbit coupling between singlet and triplet spin levels will not change the energies of spin sublevel $\varepsilon(k_a,k_b)$ sufficiently to effect a change in the population $\varepsilon(k_a,k_b)$; however, the populations perturbed by a given microwave frequency, $\omega_o(k_a,k_b)$, is more complex than in the simple one-dimensional case. Indeed in order to fully describe the effects, again knowledge of the two-dimensional spin-orbit interaction is required. Several limiting cases, however, are relatively easy to deal with.

First, when spin-orbit coupling along k_b can be neglected, the separation between triplet spin sublevel bands along k_b for any one value of k_a is constant, and hence $\omega_o(k_a,k_b)$ is constant for a given k_a. In the weak scattering limit the population perturbed by a microwave field of frequency $\omega_o(k_a,k_b)$ is simply the sum over the states k_b evaluated at k_a.

$$N(\omega) = \sum_b N(k_a,k_b) \tag{2.41}$$

Thus, the intensity of a microwave transition at a frequency $\omega_o(k_a,k_b)$ is given simply by the total population along one wave vector direction k_b from the bottom of the band to $k_b = \pm\pi/b$.

Second, when spin-orbit coupling results in an anisotropy in the zero-field splitting along both directions $\vec{a}$ and $\vec{b}$, the intensity of the

microwave frequency becomes the convolution of populations at many points on the $k_a k_b$ surface. Generally speaking, ω will be constant between spin sublevels along some curved contour which is a complex function of both the two-dimensional spin orbit and intermolecular interactions. If the spin orbit interaction along $\vec{b}$ is small compared to along $\vec{a}$, the contour of equal $\omega(k_a k_b)$'s across the surface $k_a k_b$ is relatively constant in the k_b density of states function and the line shape function reflects principally the functionality in the density of states function along k_a. Obviously when the spin orbit coupling along $\vec{a}$ and $\vec{b}$ becomes comparable and $4\beta_b \simeq 4\beta_a$, the line shape function can no longer give easily interpretable results. It is important to note that in all the above cases no additional width $\tau(k)$ is introduced explicitly by the two-dimensional interactions via averaging of the microwave frequencies since the electron spin orientation is conserved[40] for all translational equivalent exchange interactions.

III. Summary

(1) We have attempted to explain the effects of phonon-exciton scattering on the migration of coherent Frenkel excitons and have related these effects to experimentally observable phenomena. Specifically, we have derived expressions for the zero-field electron spin resonance line shape functions for triplet exciton band-to-band transitions. In one-dimensional crystals these depend intimately upon the details of phonon-exciton scattering. The problem has been considered in three regions which are determined by

the relative magnitudes of the phonon and exciton dispersions. In the narrow band limit the exciton dispersion is taken to be smaller than the phonon dispersion and at low temperatures where only the acoustic phonon branch is populated, it was found that the exciton bands suffer uniform scattering in so far as the scattering has no dependence on the exciton wave vector. Furthermore, the magnitude of the scattering was found to be dominated by the population of the phonon states which have the slowest group velocities and whose group velocities match the exciton velocities. Although the scattering reduces the coherence length of the excitons uniformly for all k states, long range energy migration might not be greatly impaired since scattering was found to occur only to nearby k states. The temperature dependence of the scattering in this limit is given by the Planck distribution function for the slowest phonon states. Uniform scattering of the exciton k states results in a uniform contribution to the electron spin T_2 of the individual wave vector states comprising the band-to-band transition. As the temperature is increased, the increased scattering results in broadening of the entire exciton band-to-band transition in a manner that depends on the exciton band width, the energy of the slowest group velocity phonon states, and on the exciton and phonon density of states functions.

(2) In the intermediate region, the exciton and acoustic phonon dispersions were taken to be approximately equal. In this case, the group velocity of the phonons in the linear section of the phonon dispersion will match the group velocity of excitons around the center of the exciton band, resulting

in a large scattering rate for the excitons around $k = \pm\pi/2a$. States near $k = 0$ and $\pm\pi/a$ were found to behave in a manner similar to those in the narrow band limit. In terms of long range energy migration this may prove most unfavorable since the fastest states are scattered the most frequently. However, in this case as above, scattering can only occur to nearby k states, and therefore long range transport of energy may still occur although the coherence length is significantly reduced. In terms of the electron spin exciton band-to-band transition, at temperatures in which the linear part of the phonon band is highly populated, the center of the band-to-band transition can be exchange narrowed while the wings can remain broad.

(3) In the broad band limit, the dispersion of the exciton band was taken to be greater than the dispersion of the acoustic phonon branch. In this case, no phonons with group velocities equal to the exciton group velocities near the center of the band are available; hence, the fastest excitons suffer the least scattering although exciton states near $k = 0$ and $\pm\pi/a$ are rapidly scattered. From the point of view of long range energy migration, this case is the most favorable. The exciton band-to-band transition will have very sharp wings due to exchange narrowing caused by rapid scattering near $k = 0$ and $\pm\pi/a$.

(4) Finally, additional factors which affect the exciton band-to-band transition have been considered. These include the effects of intramolecular spin-orbit coupling, an external magnetic field, multi-dimensional exciton interactions in the spin-orbit coupled singlet states and multi-dimensional exciton interactions in the triplet state.

IV. Acknowledgement

This work was supported in part by a grant from the National Science Foundation and in part by the Inorganic Materials Research Division of the Lawrence Berkeley Laboratory under the auspices of the U. S. Atomic Energy Commission.

References

1. J. Frenkel, Phys. Rev. 37, 17, 1276 (1931).
2. T. Holstein, Ann. Phys. (N.Y.) 8, 343 (1959); M. Grover and R. Silbey, J. Chem. Phys. 52, 2099 (1970); 54, 4843 (1971).
3. R. W. Munn and W. Siebrand, J. Chem. Phys. 52, 47 (1970).
4. A. S. Davydov, Theory of Molecular Excitons (McGraw-Hill, New York, 1962).
5. F. Bloch, Z. Physik 52, 555 (1928); C. Kittel, Quantum Theory of Solids (Wiley and Sons, New York, 1963).
6. J. M. Ziman, Principles of the Theory of Solids (Cambridge University Press, Cambridge, 1972) pp. 91-96.
7. W. Feller, An Introduction to Probability Theory and Its Applications, Vol. I-II (Wiley, New York, 1966).
8. M. D. Fayer and C. B. Harris, Phys. Rev. XX, XXXX (1973).
9. G. H. Wannier, Phys. Rev. 52, 191 (1937); J. C. Slater, Phys. Rev. 76, 1552 (1949); 87, 807 (1952).
10. G. F. Koster and J. C. Slater, Phys. Rev. 95, 1167 (1954); 96, 1208 (1954).
11. V. L. Broude and E. I. Rashba, Sov. Phys. Solid State 3, 1415 (1962); E. I. Rashba, Sov. Phys. Solid State 5, 757 (1963).
12. H. Hong and G. W. Robinson, J. Chem. Phys. 52, 825 (1970); D. P. Craig and M. R. Philpott, Proc. Roy. Soc. A 290, 583 (1965).
13. M. G. Richards, J. Pope and A. Widom, Phys. Rev. Lett. 29, 708 (1972); A. Widom and M. G. Richards, Phys. Rev. A 6, 1196 (1972).
14. A. H. Francis and C. B. Harris, Chem. Phys. Lett. 9, 181 (1971).

15. P. Reineker and H. Haken, Z. Physik 250, 300 (1972); H. Haken and P. Reineker, Z. Physik 249, 253 (1972).

16. C. A. Hutchison, Jr., and B. W. Mangum, J. Chem. Phys. 34, 908 (1961).

17. J. Jortner, S. A. Rice and J. L. Katz, J. Chem. Phys. 42, 309 (1965); G. C. Nieman and G. W. Robinson, J. Chem. Phys. 39, 1298 (1963); R. M. Hochstrasser and J. D. Whiteman, J. Chem. Phys. 56, 5945 (1972).

18. C. P. Slichter, Principles of Magnetic Resonance (Harper & Row, New York, 1963) p. 32.

19. J. Hoshen and J. Jortner, J. Chem. Phys. 56, 933, 4138, 5550 (1972); H. Hong and G. W. Robinson, J. Chem. Phys. 52, 825 (1970); 54, 1369 (1971); D. M. Burland and G. W. Robinson, J. Chem. Phys. 66, 257 (1970).

20. D. D. Thomas, H. Keller and H. M. McConnell, J. Chem. Phys. 39, 2321 (1963); D. D. Thomas, A. W. Merkl, A. F. Hildebrandt and H. M. McConnell, J. Chem. Phys. 40, 2588 (1964).

21. Von D. Haarer and H. C. Wolf, Molecular Crystals and Liquid Crystals 10, 359 (1970).

22. A. H. Francis and C. B. Harris, Chem. Phys. Lett. 9, 188 (1971).

23. D. S. McClure, J. Chem. Phys. 17, 665 (1949); 20, 682 (1952).

24. F. Bloch, Phys. Rev. 70, 460 (1946).

25. A. Abragam, The Principles of Nuclear Magnetism (Oxford Press, London, 1961).

26. M. S. DeGroot, I. A. M. Hesselmann and J. H. Van der Waals, Mol. Phys. 12, 259 (1967).

27. C. B. Harris, J. Chem. Phys. 54, 972 (1971).

28. R. Kubo and K. Tomita, J. Phys. Soc. Japan 9, 888 (1954); R. Kubo, J. Phys. Soc. Japan 9, 935 (1954); P. W. Anderson, J. Phys. Soc. 9, 316 (1954).

29. M. L. Goldberger and K. M. Watson, Collision Theory (Wiley, New York, 1964).

30. The effects of coherent and incoherent exciton migration on spin resonance absorption has been treated from a phenomenological approach in the work of Haken and Reineker.[15] However, the form of phonon-exciton coupling was not explicitly incorporated into the magnetic Bloch equations but rather incorporated into the equations of motion via a Gaussian Markov fluctuation of the exchange integral. Their approach has the distinct advantage in treating the intermediate region in so far as it is more ameanable to solution. Specific information, however, regarding phonon-exciton coupling is not displayed.

31. Z. G. Soos and H. M. McConnell, J. Chem. Phys. 43, 3780 (1965); H. Sternlicht and H. M. McConnell, J. Chem. Phys. 35, 1796 (1961); Z. G. Soos, J. Chem. Phys. 44, 1729 (1966).

32. R. W. Munn, J. Chem. Phys. 52, 64 (1970).

33. Ziman, op. cit., pp. 27-36.

34. R. C. Tolman, The Principles of Statistical Mechanics (Oxford University Press, Oxford, 1967) p. 512.

35. P. Debye, Ann. Phys. 39, 789 (1912); J. M. Ziman, op. cit., pp. 43-46.

36. G. S. Pawley and E. A. Yeats, Solid State Commun. 7, 385 (1969).

37. L. van Hove, Phys. Rev. 89, 1189 (1953).

38. M. D. Fayer and C. B. Harris, unpublished results.

39. A. H. Francis and C. B. Harris, J. Chem. Phys. 55, 3595 (1971).

40. D. L. Dexter, J. Chem. Phys. 21, 836 (1953).

Figure Captions

Figure 1 (a) Energy dispersion of the three magnetic sublevels τ_x, τ_y and τ_z in the triplet exciton band T_1 in the absence of spin-orbit coupling.

(b) Energy dispersion of the triplet magnetic sublevel bands including selective spin-orbit coupling of τ_x to higher singlet states.

The energy scale is purely schematic and is used for illustrative purposes only.

Figure 2 Calculated electron spin resonance band-to-band transitions in the absence of selective spin-orbit coupling for various triplet band widths 4β. Each curve represents the sum of contributions from a Boltzmann distribution over the individual k states. Each value of k in the band-to-band transition has associated with it an intrinsic line width ΔF^p and a group velocity dependent line width, ΔF^k. ΔF^k is listed for the states at the center of the band ($k = \pm\pi/2a$) for the various band widths illustrated. The intensities of the spectra are adjusted to have the same maximum height and are not normalized relative to one another.

Figure 3 Calculated electron spin resonance triplet exciton band-to-band transitions in the absence of selective spin-orbit coupling

for several temperatures. In addition to the temperature dependence these curves illustrate the effect of different group velocity dependent line widths and the dependence on the number of k states in the exciton bands. Each spectrum is adjusted to have the same maximum height.

Figure 4 The relative magnitudes of the exciton and acoustic phonon dispersions.

(a) The narrow exciton band limit where the phonon group velocity matches the exciton group velocity in the non-linear region of the phonon dispersion.

(b) The intermediate region where the phonon group velocity in the linear region of the phonon dispersion matches the exciton velocities around the center of the exciton band.

(c) The broad band limit where the phonon group velocities match the exciton velocities near the top and bottom of the exciton band.

Figure 5 Calculated electron spin resonance triplet exciton band-to-band transitions for several exciton band widths with selective spin-orbit coupling. The exciton and phonon dispersions are in the narrow band limit and a Boltzmann distribution characterizes the population. The shape of each of the curves

reflects the exciton band width, exciton density of states function, and the rate of phonon-exciton scattering. The total area under each of the spectra has been normalized.

Figure 6 Calculated electron spin resonance triplet exciton band-to-band transitions with selective spin-orbit coupling to the individual triplet spin sublevels in the narrow exciton band limit. The curves are for several exciton band widths and several temperatures. ΔF is the half width at half height of the individual wave vector states comprising the exciton band. The spectra show the broadening effect due to increased phonon-exciton scattering with increasing temperature. The total area under each of the spectra has been normalized.

Figure 7 Exciton coherence time, $\tau(k')$, as a function of temperature in the broad exciton band limit for the exciton state k' which has its group velocity $V_g(k')$ equal to the group velocity of phonons in the linear region of the phonon dispersion.

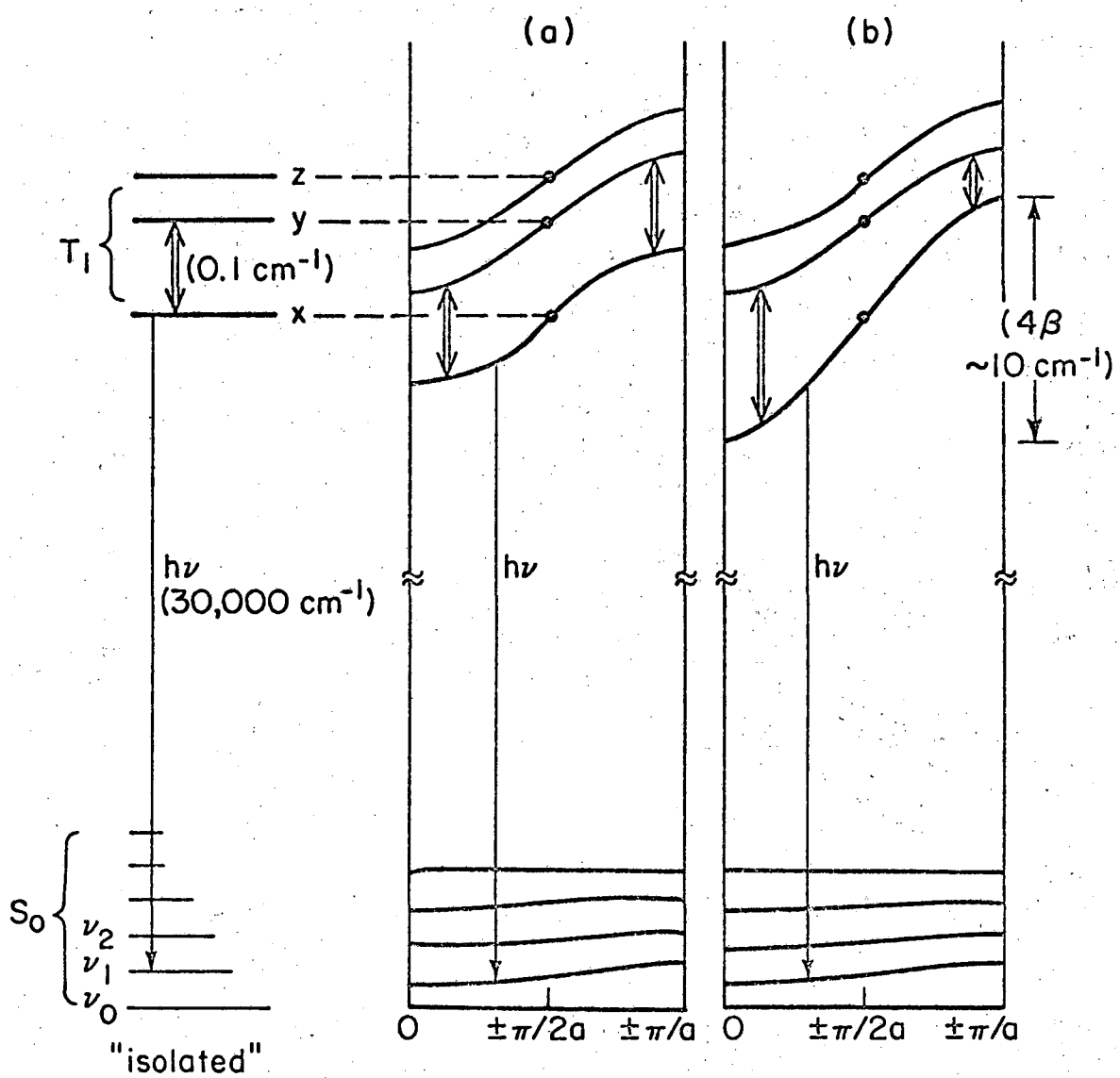

Triplet Spin-sublevel Bands
(a) without spin-orbit coupling
(b) with spin-orbit coupling

XBL 734-383

Fig. 1

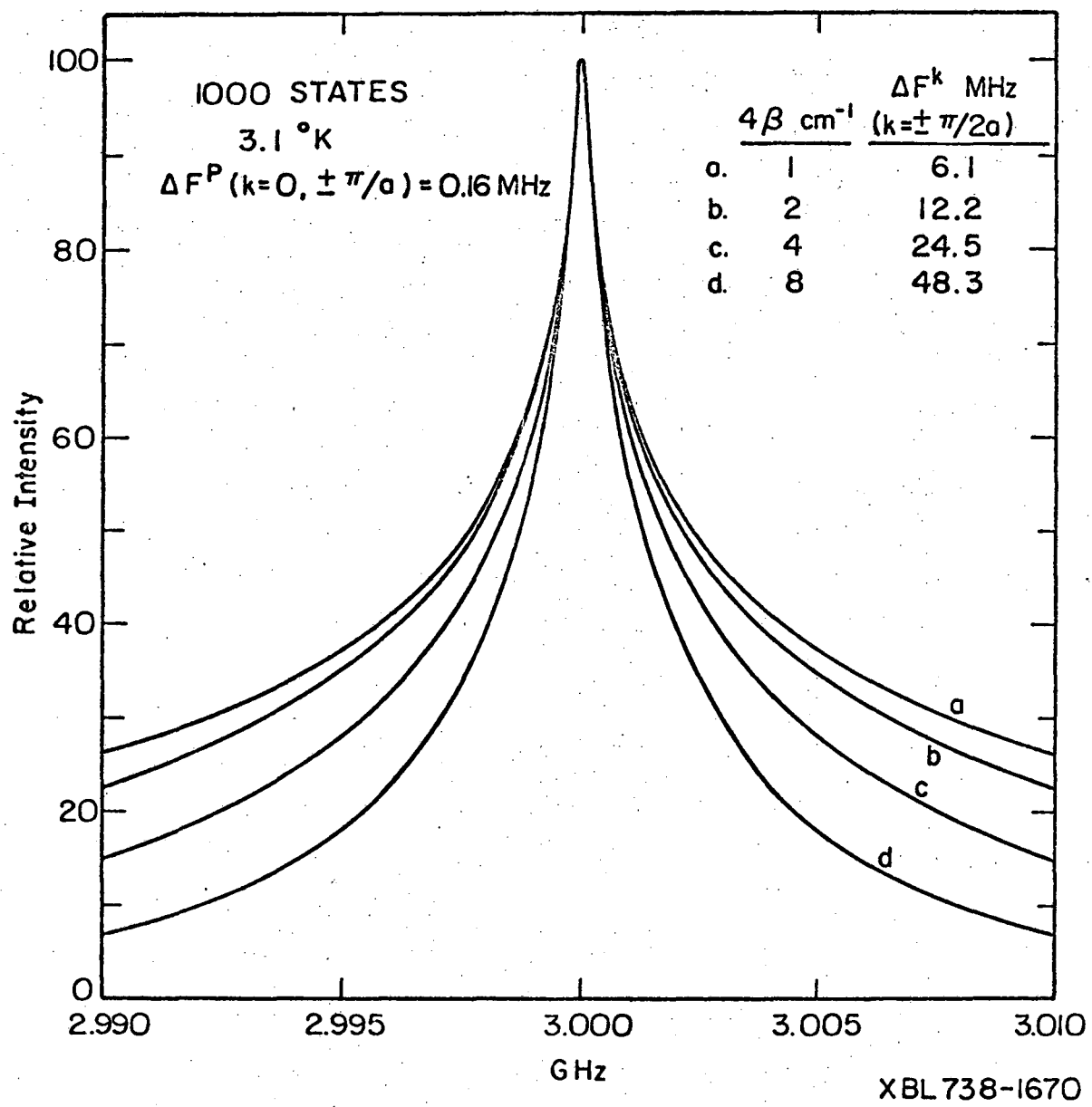
1000 STATES
3.1 °K
ΔF^P (k=0, ± π/a) = 0.16 MHz
4β cm^-1
ΔF^k MHz (k=± π/2a)
a. 1 6.1
b. 2 12.2
c. 4 24.5
d. 8 48.3
Relative Intensity
100
80
60
40
20
0
2.990
2.995
3.000
3.005
3.010
GHz
a
b
c
d
XBL 738-1670

Fig. 2

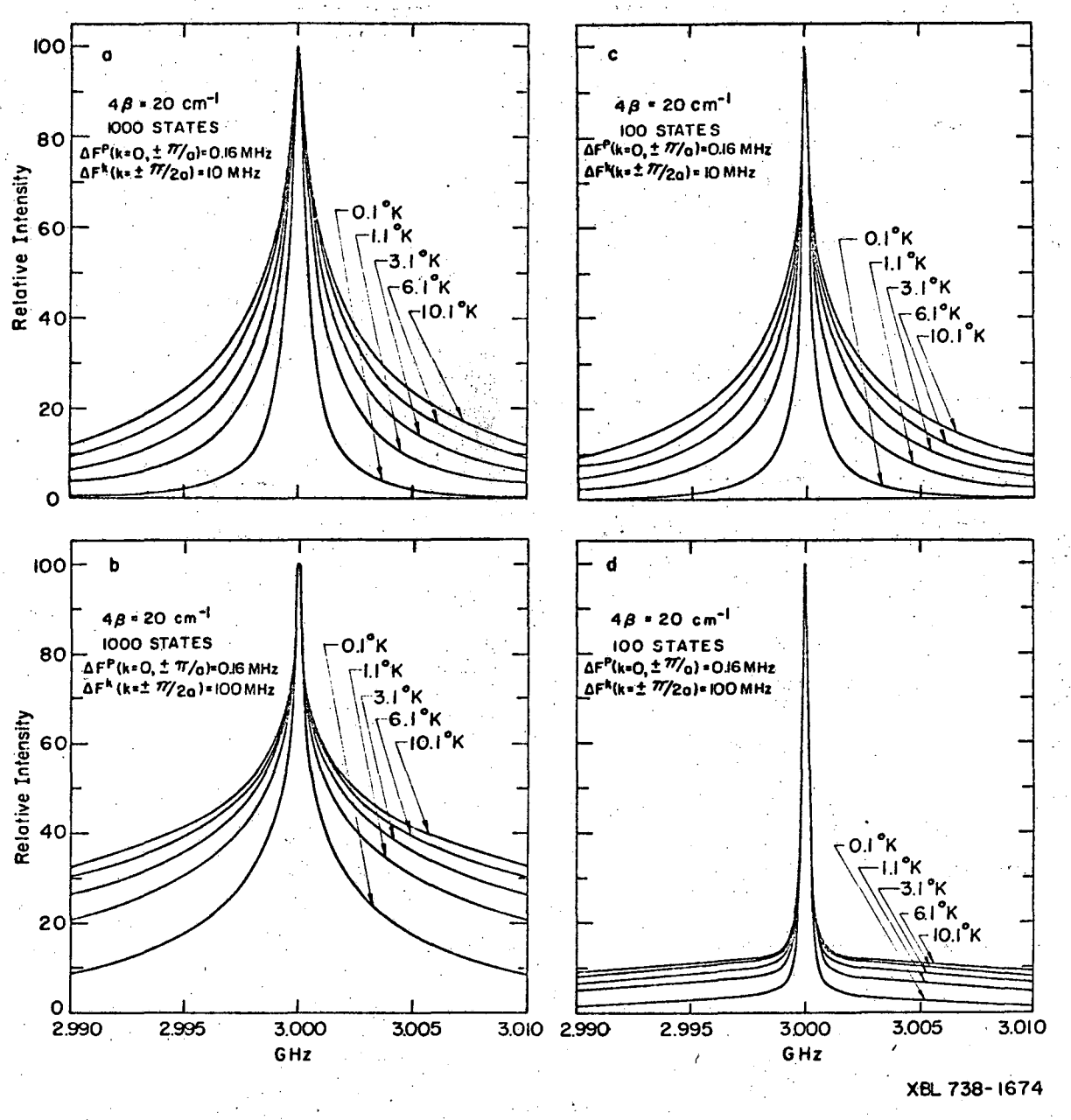
a
4β = 20 cm⁻¹
1000 STATES
ΔF^P(k=0, ± π/a)=0.16 MHz
ΔF^k(k=± π/2a)=10 MHz
0.1°K
1.1°K
3.1°K
6.1°K
10.1°K
c
4β = 20 cm⁻¹
100 STATES
ΔF^P(k=0, ± π/a)=0.16 MHz
ΔF^k(k=± π/2a)=10 MHz
b
4β = 20 cm⁻¹
1000 STATES
ΔF^P(k=0, ± π/a)=0.16 MHz
ΔF^k(k=± π/2a)=100 MHz
d
4β = 20 cm⁻¹
100 STATES
ΔF^P(k=0, ± π/a)=0.16 MHz
ΔF^k(k=± π/2a)=100 MHz
Relative Intensity
0
20
40
60
80
100
2.990
2.995
3.000
3.005
3.010
GHz
XBL 738-1674

Fig. 3

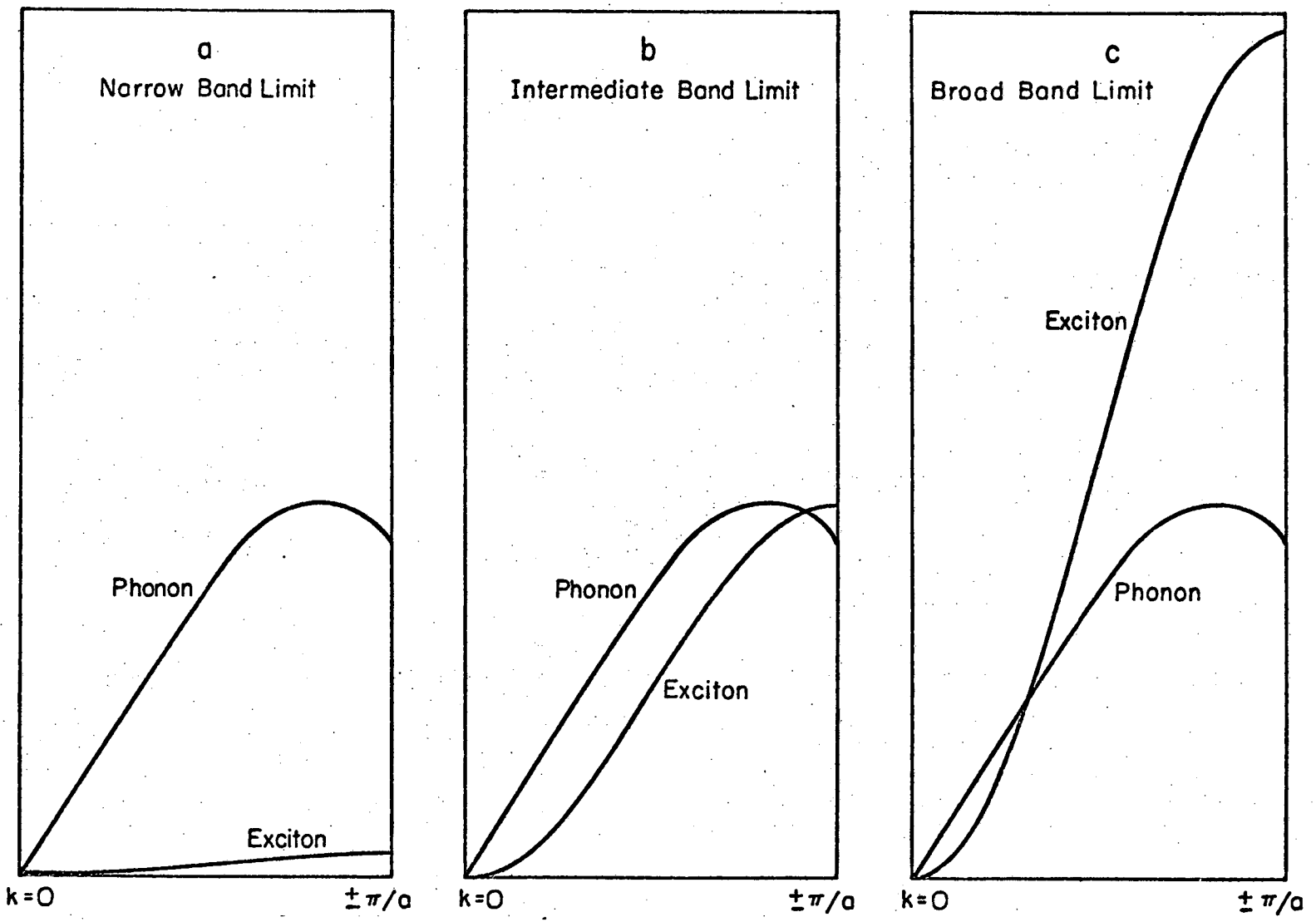

XBL738-1671

Fig. 4

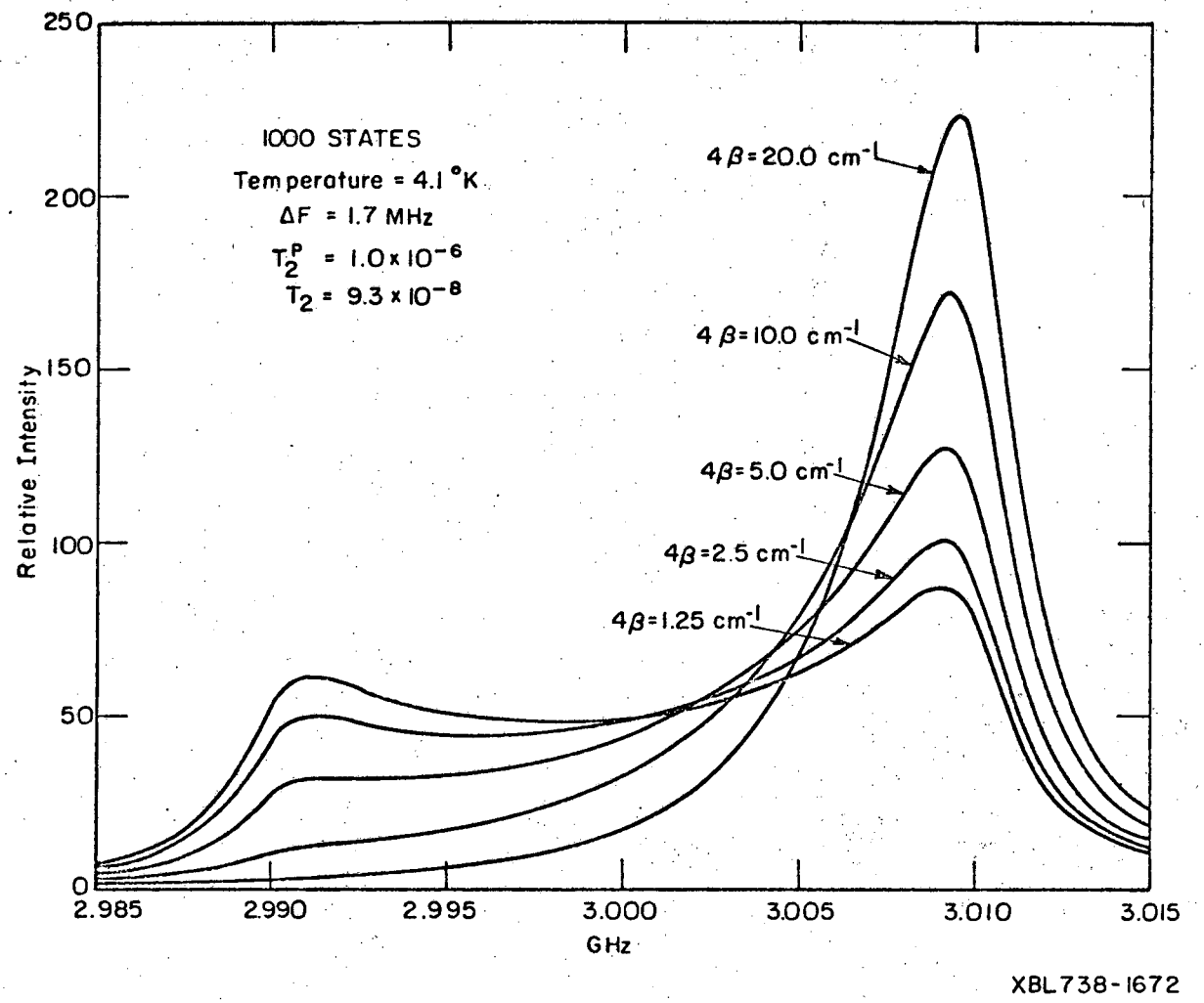
1000 STATES
Temperature = 4.1 °K
ΔF = 1.7 MHz
T_2^p = 1.0 x 10^{-6}
T_2 = 9.3 x 10^{-8}
4β = 20.0 cm^{-1}
4β = 10.0 cm^{-1}
4β = 5.0 cm^{-1}
4β = 2.5 cm^{-1}
4β = 1.25 cm^{-1}
Relative Intensity
250
200
150
100
50
0
2.985
2.990
2.995
3.000
3.005
3.010
3.015
GHz
XBL738-1672

Fig. 5

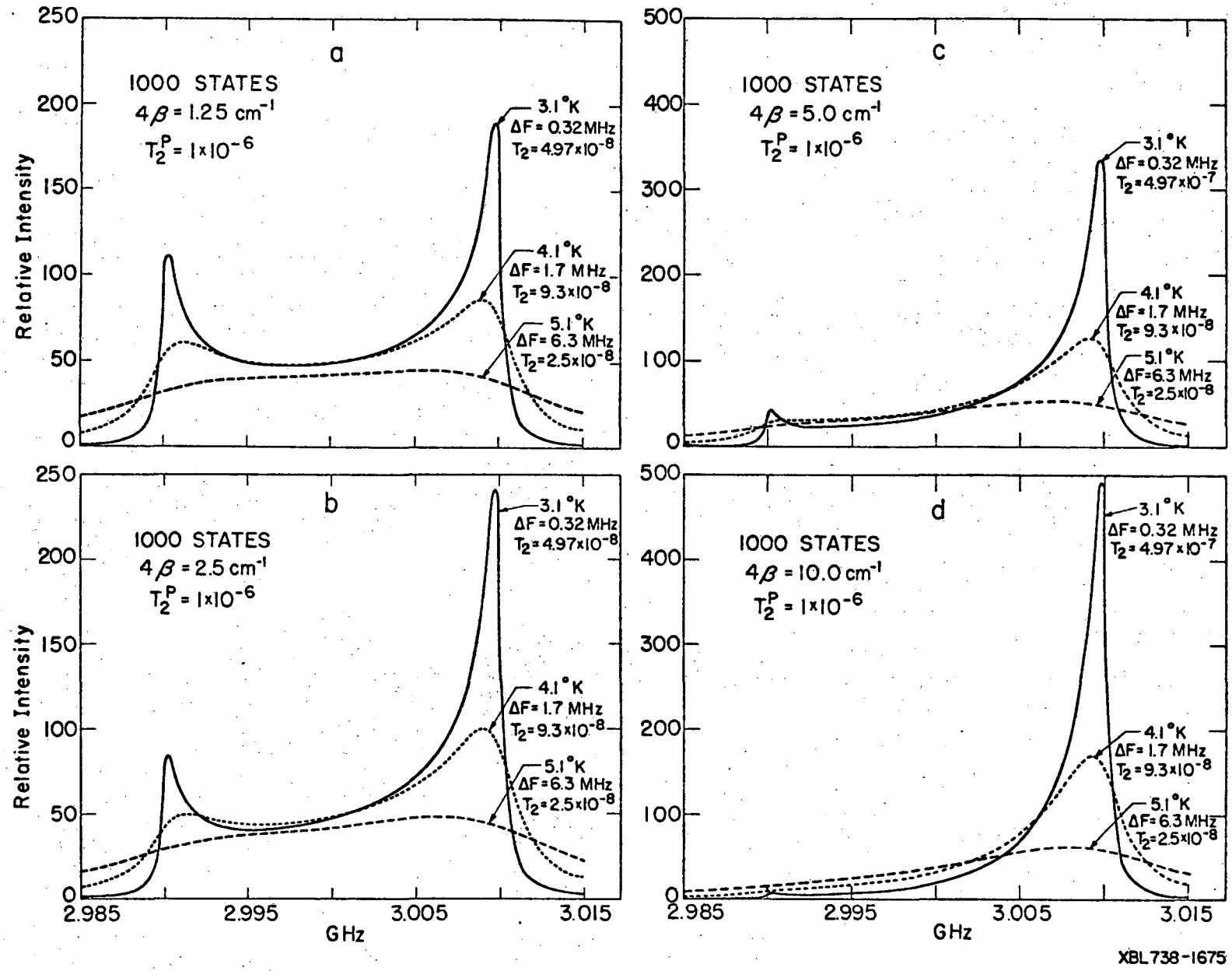
a
1000 STATES
4β = 1.25 cm⁻¹
T₂ᴾ = 1×10⁻⁶
3.1°K
ΔF = 0.32 MHz
T₂ = 4.97×10⁻⁸
4.1°K
ΔF = 1.7 MHz
T₂ = 9.3×10⁻⁸
5.1°K
ΔF = 6.3 MHz
T₂ = 2.5×10⁻⁸
b
1000 STATES
4β = 2.5 cm⁻¹
T₂ᴾ = 1×10⁻⁶
c
1000 STATES
4β = 5.0 cm⁻¹
T₂ᴾ = 1×10⁻⁶
T₂ = 4.97×10⁻⁷
d
1000 STATES
4β = 10.0 cm⁻¹
T₂ᴾ = 1×10⁻⁶
Relative Intensity
GHz
2.985
2.995
3.005
3.015
XBL 738-1675

Fig. 6

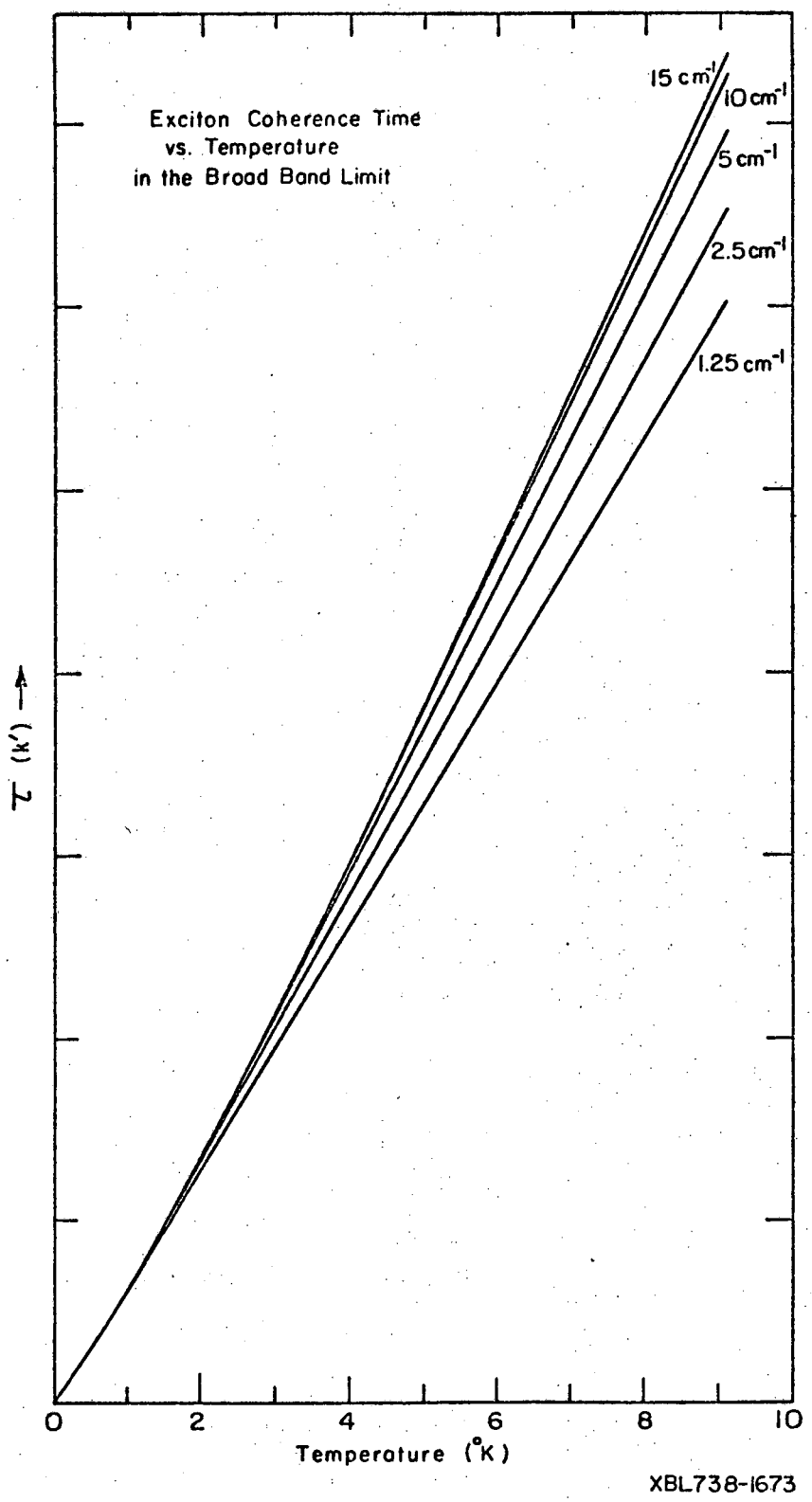
Exciton Coherence Time
vs. Temperature
in the Broad Band Limit
15 cm⁻¹
10 cm⁻¹
5 cm⁻¹
2.5 cm⁻¹
1.25 cm⁻¹
τ (ps)
0
2
4
6
8
10
Temperature (°K)
XBL738-1673

Fig. 7

LEGAL NOTICE

This report was prepared as an account of work sponsored by the United States Government. Neither the United States nor the United States Atomic Energy Commission, nor any of their employees, nor any of their contractors, subcontractors, or their employees, makes any warranty, express or implied, or assumes any legal liability or responsibility for the accuracy, completeness or usefulness of any information, apparatus, product or process disclosed, or represents that its use would not infringe privately owned rights.

TECHNICAL INFORMATION DIVISION
LAWRENCE BERKELEY LABORATORY
UNIVERSITY OF CALIFORNIA
BERKELEY, CALIFORNIA 94720